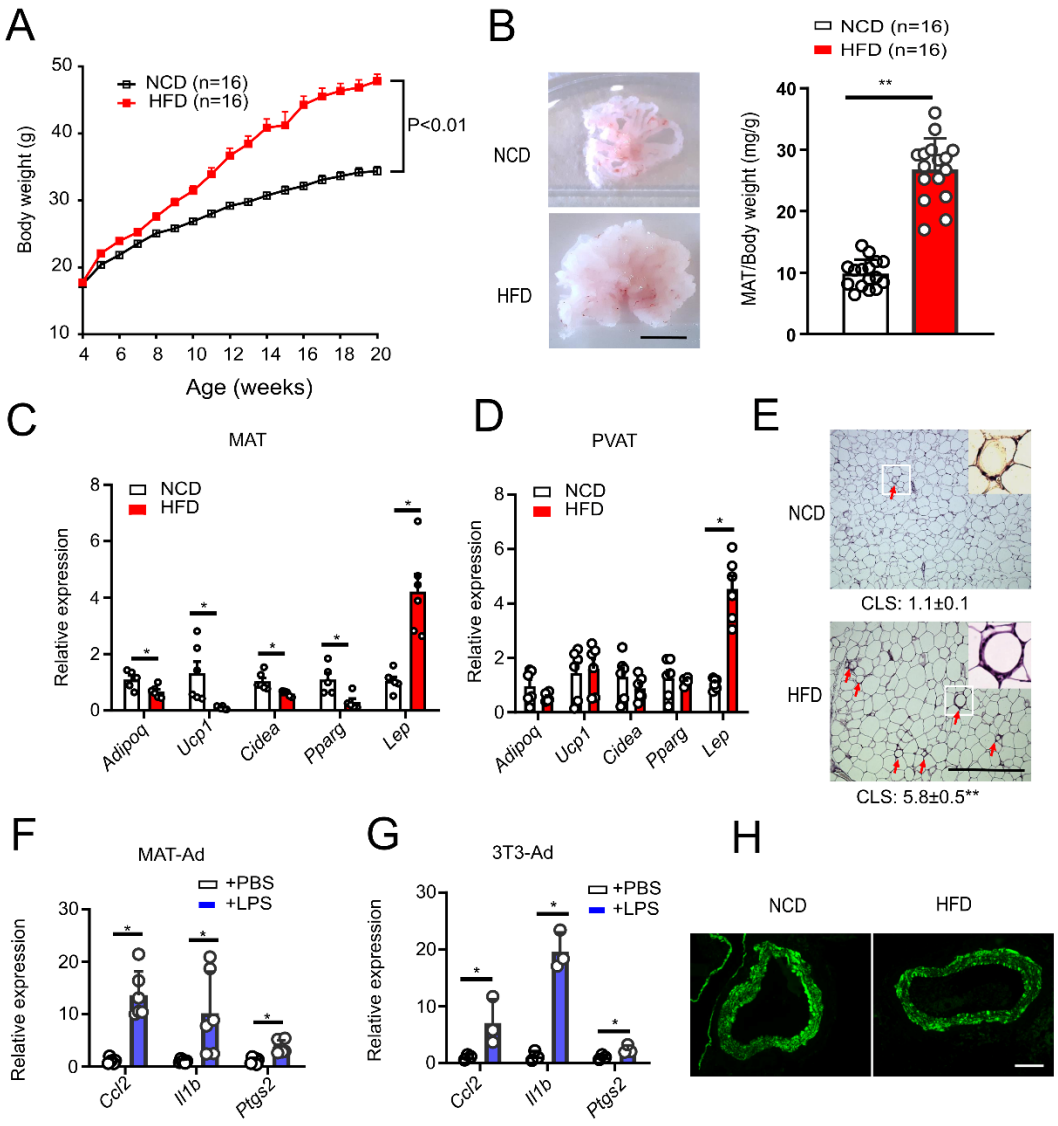

Figure S1. Obesity, hypertrophic adipocytes, and inflammation in MAT of HFD-fed mice and in LPS-challenged MAT/3T3-derived adipocytes. A, Body weight changes of mice fed a normal chow diet (NCD) or a high fat diet (HFD). $^{**}P<0.01$ as determined by the Repeated Measures in General Linear Model of SPSS. **B**, Representative images of mesenteric adipose tissue (MAT) fat depots and quantification of MAT weight. Scale bar, 10 mm. **C**, Real-time qPCR-determined relative expression of adiponectin (*Adipoq*), *Ucp1*, *Cidea*, *Pparg*, and leptin (*Lep*) mRNAs in MAT. **D**, Real-time qPCR-determined relative expression of *Adipoq*, *Ucp1*, *Cidea*, *Pparg*, and *Lep* mRNAs in AA-PVAT. n=6. **E**, Representative images of MAT stained with CD68 antibody (red arrows, brown CD68-positive cells) by DAB and the number of crown-like structures (CLS) surrounding inflamed adipocytes. Scale bar indicates 500 μm for the low magnification, whereas 100 μm for the insets of higher magnification. Numbers under each micrograph are mean ± SEM of CLS counted. n=6. **F**, Real-time qPCR-determined relative expression of pro-inflammatory genes including *Ccl2*, *Il1b*, and *Ptgs2* (COX-2). Primary MAT-derived adipocytes (MAT-Ad) were incubated with PBS or lipopolysaccharide (LPS, 1 μg/ml) for 24 h and subjected to total RNA isolation and PCR assays. Data represent mean ± SEM. $^{*}P<0.05$ vs the corresponding PBS value (unpaired 2-tailed *t* test); n=6. **G**, Relative mRNA expression of *Ccl2*, *Il1b*, and *Ptgs2* in PBS- or LPS-stimulated 3T3-L1 differentiated adipocytes (3T3-Ad). Data represent mean ± SEM. $^{*}P<0.05$ vs the corresponding PBS value (unpaired 2-tailed t test); n=3. **H**, Immunohistochemical staining for smooth muscle α-actin (green) in the abdominal aorta (AA). Scale bar, 100 μm**.** All data (B-G) are presented as mean ± SEM, $^{*}P<0.05$ and $^{**}P<0.01$ vs the corresponding NCD value (unpaired 2-tailed *t* test).

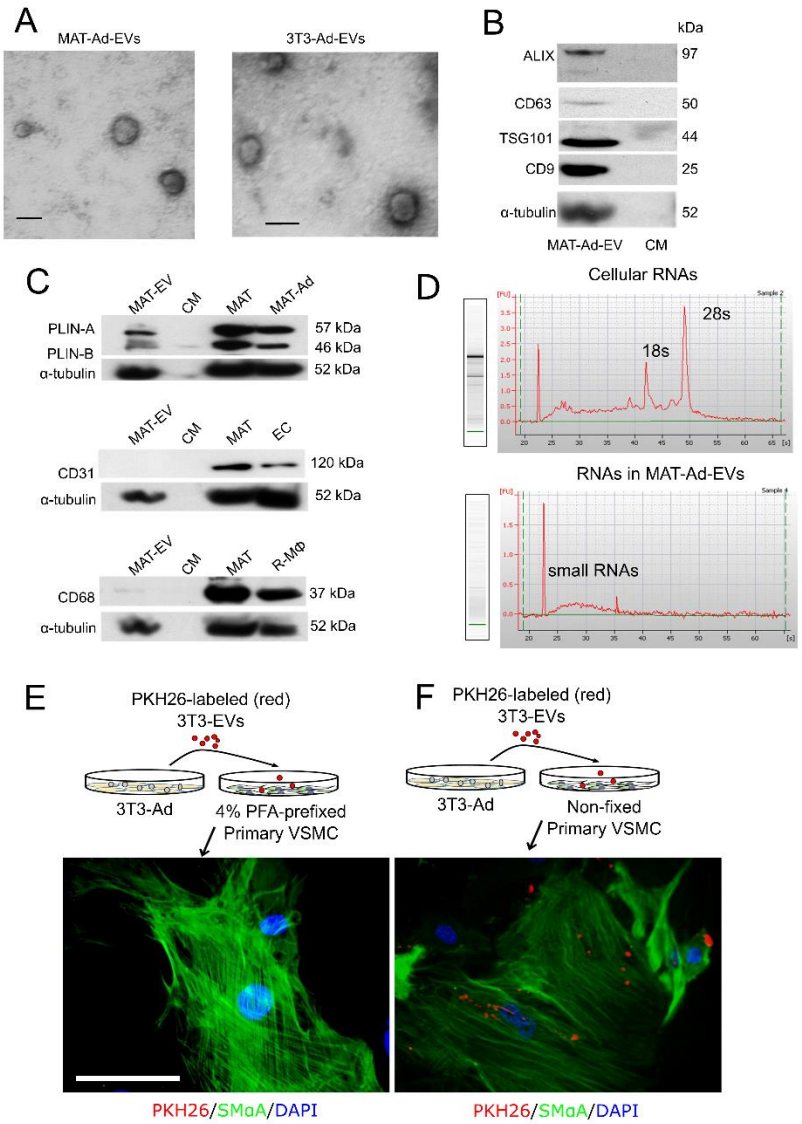

Figure S2. Primary adipocytes and 3T3-L1-derived adipocytes secrete extracellular vesicles containing miRNAs. A, Electron microscopy analysis of extracellular vesicles (EVs) secreted by primary MAT-derived adipocytes (MAT-Ad-EVs) and 3T3-dervied adipocytes (3T3-Ad-EVs), showing a size of approximately 50 to 100 nm in diameter. Scale bars, 100 nm. **B,** EV-related protein markers ALIX (97 kDa), CD63 (50 kDa), TSG101 (44 kDa), and CD9 (25 kDa) were detected by Western blot analysis in MAT-Ad-EVs but not in supernatant-conditioned medium (CM). TSG101, tumor susceptibility gene 101. These blots are representative of 3 independent experiments. **C**, Representative immunoblots of adipocyte marker PLIN-A/B (57/46 kDa), endothelial cell marker CD31 (120 kDa), and macrophage marker CD68 (37 kDa) expression in MAT-EV, CM, MAT, and a positive control sample (MAT-Ad, EC, and R-MΦ, respectively). EC, primary endothelial cell; R-MΦ, peritoneal resident macrophage. **D**, Characterization of total RNA, including miRNAs encapsulated in MAT-Ad-derived EVs (MAT-Ad-EVs) and the corresponding primary MAT-Ad (Cellular) by Agilent 2100 Bioanalyzer. Both gels and electropherograms are shown. Y axis of the electropherogram is arbitrary fluorescence unit intensity (FU) and X axis is migration time in seconds (s). **E** and **F**, Cellular internalization of 3T3-L1-derived EVs into murine primary VSMCs. 4%-PFA prefixed-VSMCs (E) or non-fixed VSMCs (F) were incubated with PKH67-labeled (red) exosomes for 18 h, and then were immunolabeled by FITC-conjugated α-smooth muscle actin (green) and DAPI staining of nuclei (blue). Scale bar, 100 μm. Red fluorescence was barely observed in VSMCs prefixed with 4% PFA prior to the incubation with labeled EVs, whereas punctate labelings are observed in non-fixed VSMCs.

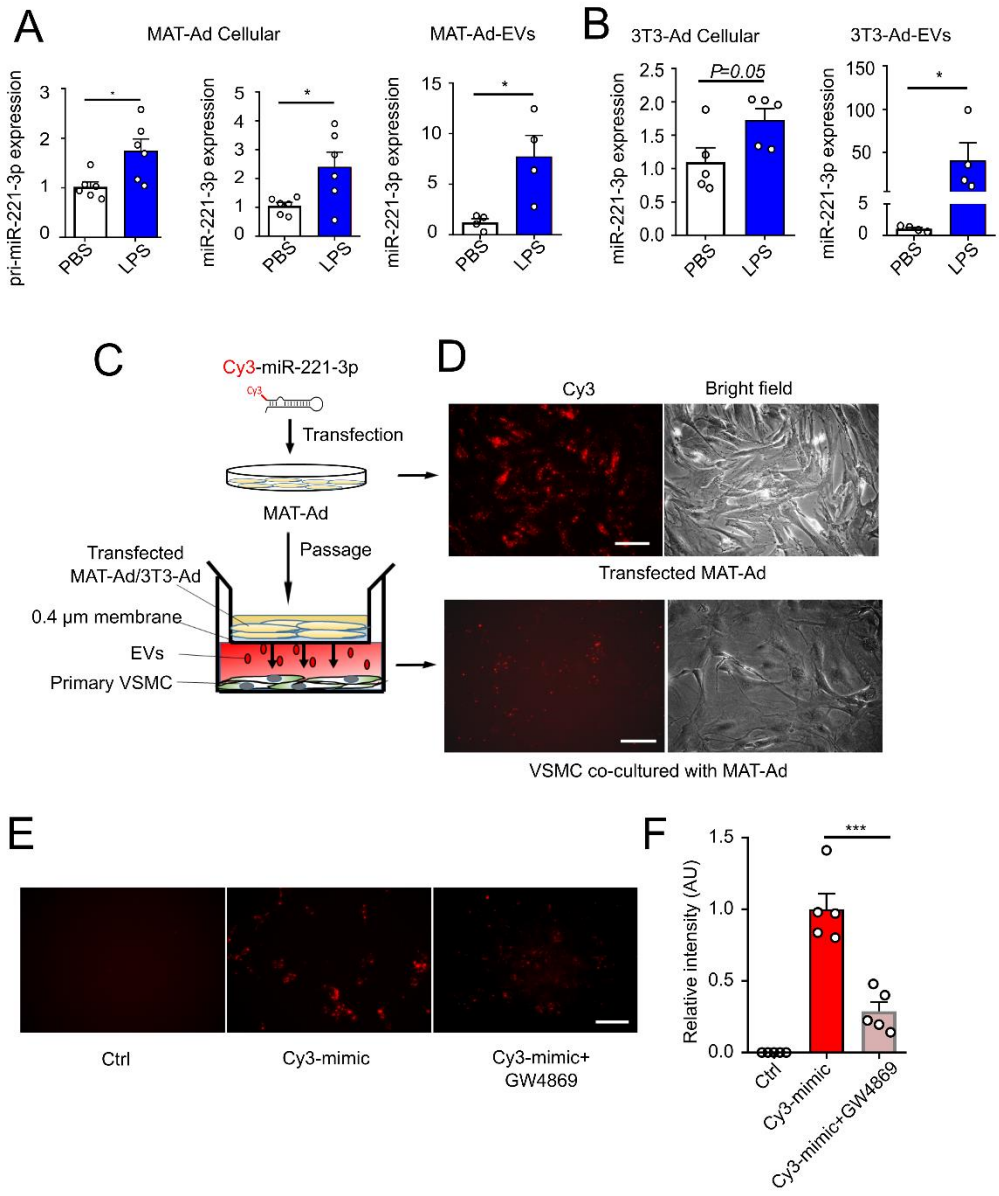

Figure S3. Differential expression and transport of miR-221-3p. A, Relative expression levels of pri-miR-221-3p and miR-221-3p in MAT-derived adipocytes (MAT-Ad) and expression of miR-221-3p in MAT-EVs. MAT-Ad cells were challenged with PBS or LPS (1 μg/ml) for 24 h and then subjected to cellular RNA or EV RNA purification. **B**, Relative expression of cellular and EV miR-221-3p in 3T3-Ad. **C,** Experimental setup of transwell co-culture assays. MAT-Ad cells transfected with Cy3-labeled miR-221-3p mimics were seeded in the upper chamber, recipient primary VSMC cells were in the bottom well (membrane pore=0.4 μm). **D**, Representative images of MAT-Ad cells transfected with Cy3-labeled miR-221-mimics (Cy3-mimic); images of recipient primary VSMC cells co-cultured with transfected MAT-Ad cells for 24 h. **E**, Immunofluorescence staining of recipient MOVAS cells co-cultured with transfected 3T3-Ad cells for 24 h. Prior to co-culture, some transfected 3T3-Ad cells were pre-treated with n-SMase inhibitor GW4869 (10 μM) for 24 h. **F**, Quantification of fluorescence intensities shown in D. The pri-miR-221-3p data were normalized to levels of endogenous GAPDH, whereas the cellular and EV miR-221-3p expression data were normalized with miR-361-5p and miR-320a, respectively. Data in A and B are presented as mean ± SEM, $^{*}P<0.05$ versus the corresponding PBS-treated cells (unpaired 2-tailed *t* test or nonparametric Kruskal-Wallis test). One-way ANOVA analysis indicates $^{***}P<0.001$ in F. Scale bars, 100 μm (D and E).

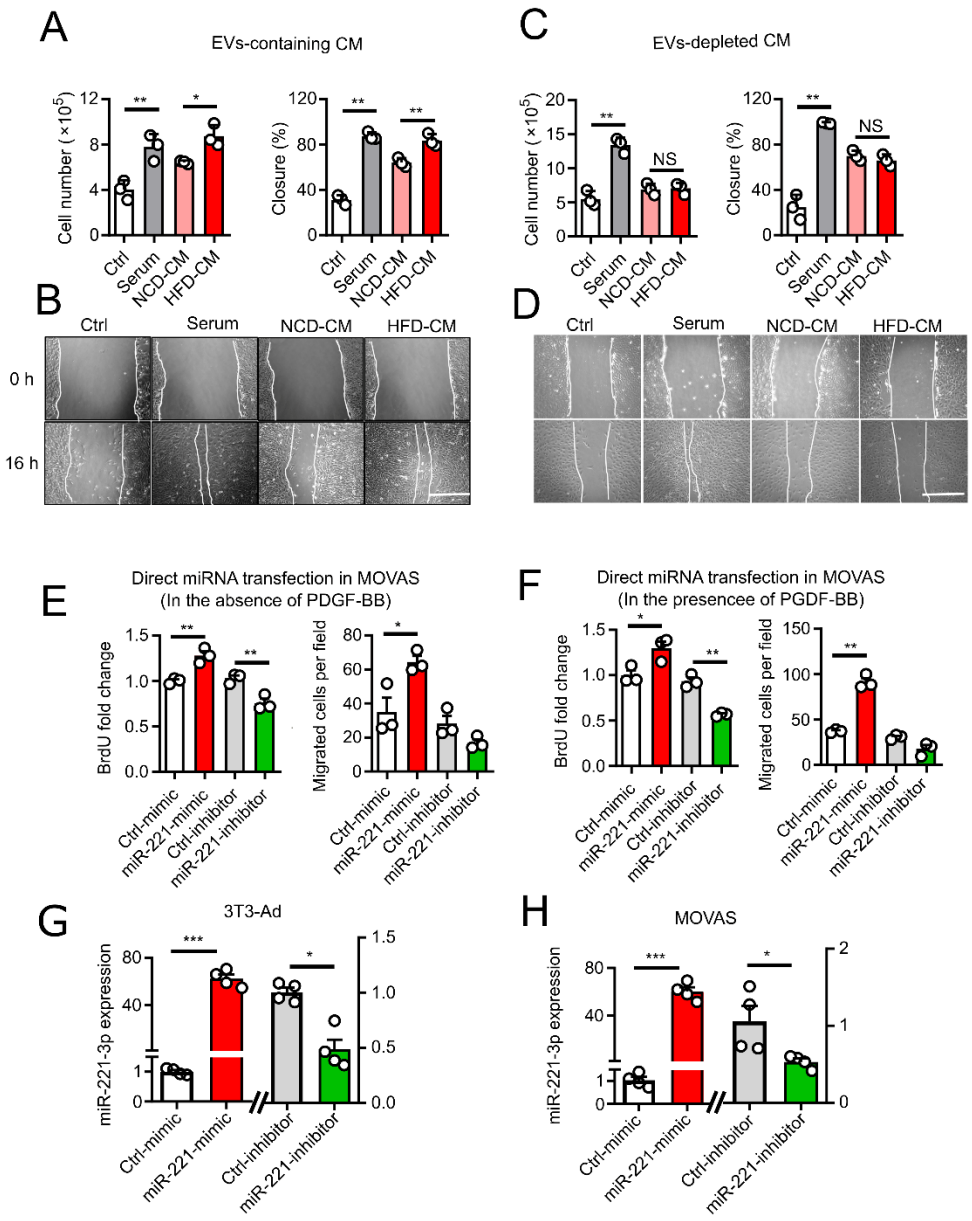

Figure S4. miR-221-3p promotes MOVAS cell growth and migration. A, MOVAS cell counting and migration assays (wound-healing) in the presence of EVs (EVs-containing CM) as described in the Methods section. Starved MOVAS cells were treated with Control (Ctrl, 0.5 % serum), 20% serum, NCD- or HFD-conditioned medium (CM) for an additional 16 h. **B,** Representative photographs showing wound healing progression from 0 to 16 h in EVs-containing CM treatment. **C**, MOVAS cell counting and migration assays (wound-healing) in the absence of EVs (EVs-depleted CM). **D**, Representative photographs showing wound healing progression from 0 to 16 h in EVs-depleted CM treatment. **E,** (left) Fold change of BrdU positive cell number/field relative to Ctrl-mimic and (right) cell migration assays (transwell, membrane pore=8 µm) in MOVAS directly transfected with miR-221-3p mimics, miR-221-3p inhibitor, or respective control miRNAs. **F**, In the presence of PDGF-BB (10 ng/ml), (left) fold change of BrdU positive cell number/field relative to Ctrl-mimic and (right) transwell migration assays in MOVAS cells directly transfected with miR-221-3p mimics, miR-221-3p inhibitor, or respective control miRNAs. **G and H,** Real-time qPCR analysis validated miR-221-3p overexpression or down-regulation in 3T3-Ad or MOVAS cells transfected with miR-221-3p mimic or miR-221-3p inhibitor, respectively. Data are averaged representatives from at least two independent experiments. $^{*}P<0.05$, $^{**}P<0.01$ and $^{***}P<0.01$ versus the corresponding NCD or Ctrl value (unpaired 2-tailed *t* test, or One-way ANOVA). NS indicates no significance. Note that different left and right y-axis scales are used in panels G and H. Bars, 500 µm (B and D).

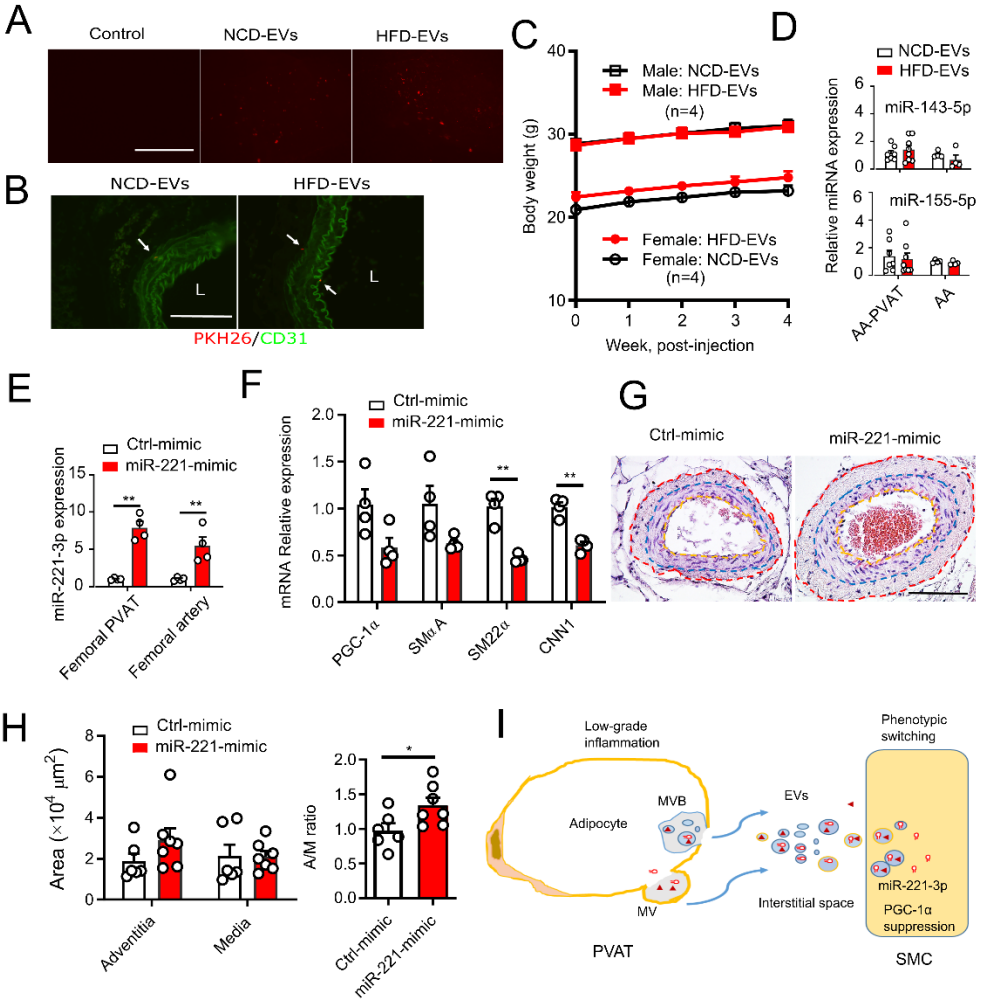

Figure S5. Modulation of miR-221-3p influences arterial phenotype in vivo. A, Appearance of PKH26-labeled EVs in MAT of lean recipient mice after 1 week from last intraperitoneal administration of either HFD-EVs or NCD-EVs. Freshly dissected MAT was spread on a slide for fluorescent visualization. Scale bar, 500 μm. **B,** Distribution of PKH26-labeled EVs (white arrows) in paraffin-embedded, CD31-immunostained abdominal aorta of lean recipient mice after 1 week from last intraperitoneal administration of either HFD-EVs or NCD-EVs. Scale bar, 100 μm. L, lumen. **C**, Body weight changes of mice treated with HFD- or NCD-EVs over the course of 4 weeks. **D**, Intraperitoneal delivery of HFD-EVs did not change expression of miR-143-5p and miR-155-5p in lean recipient abdominal aorta and PVAT. **E**, Local enforced expression of miR-221-3p after perivascular transfection of miRNA mimics in femoral arteries and PVAT. Total RNA was harvested from femoral arteries and surrounding PVAT before undergoing RT-qPCR analyses. **F**, Relative mRNA expression of selective contractile marker genes including SMαA, SM22α, and CNN1 and target gene PGC-1α in femoral arteries. Data represent mean ± SEM. $^{*}P<0.05$ versus the corresponding NCD-EV value (unpaired 2-tailed t test); 2 femoral arteries or femoral PVATs were pooled for each experiment. **G**, Histopathological analysis of representative femoral arteries by HE staining. The adventitial area is demarcated with the red and blue dotted lines and medial area is between the blue and yellow dotted lines. Scale bar, 100 μm. **H**, Quantification of femoral arterial adventitial area, medial area, and adventitia-to-media (A/M) ratio. **I,** Schematic diagram of EV-miR-221-3p pathway in PVAT. In the context of obesity-associated low-grade inflammation, perivascular adipocyte-derived miRNA-containing EVs act as signaling mediators in PVAT-initiated inward inflammatory cascades, which in turn triggers smooth muscle cells to undergo phenotypic switching. PVAT adipocytes secrete EVs enriched with miR-221-3p, which are transported to medial smooth muscle cells. miR-221-3p down-regulates the expression of contractile and target genes, leading to arterial de-differentiation and dysfunction. MVB, multivesicular body; MV, microvesicle; EVs, extracellular vesicles; PVAT, perivascular adipose tissue; SMC, smooth muscle cell; PGC-1α, peroxisome proliferator-activated receptor gamma coactivator 1alpha.